Supporting Information

Junshu Lin,[1,2] Quan Wang,[2] Xiaoyu Wang,[2] Yunyao Zhu,[2] Xi Zhou,[1,*] and Hui Wei[2,3,*]

[1]Department of Biomaterials, College of Materials, Xiamen University, Xiamen, Fujian 361005, China.

[2]Department of Biomedical Engineering, College of Engineering and Applied Sciences, Nanjing National Laboratory of Microstructures, Jiangsu Key Laboratory of Artificial Functional Materials, Chemistry and Biomedicine Innovation Center (ChemBIC), Nanjing University, Nanjing, Jiangsu 210093, China.

[3]State Key Laboratory of Analytical Chemistry for Life Science and State Key Laboratory of Coordination Chemistry, School of Chemistry and Chemical Engineering, Collaborative Innovation Center of Chemistry for Life Sciences, Nanjing University, Nanjing, Jiangsu 210023, China.

Email: xizhou@xmu.edu.cn; weihui@nju.edu.cn; Web: http://weilab.nju.edu.cn; **Tel:** +86-25-83593272; **Fax:** +86-25-83594648.

Table of contents

bar shows the standard deviation of three independent measurements.

Figure S4. Kinetic curves of A_{450} for monitoring the catalytic reaction of 2 mM OPD and 10 mM H_2O_2 in the presence of 5 μg/mL different noble metal nanozymes.

Figure S5. Typical absorption spectra for monitoring the catalytic oxidation of OPD in the presence of AuPd nanozymes with various concentrations of (a) GSH, (b) DTT, (c) MS, (d) MA, and (e) ME.

Figure S6. Typical absorption spectra for monitoring the catalytic oxidation of OPD in the presence of AuPt nanozymes with various concentrations of (a) GSH, (b) DTT, (c) MS, (d) MA, and (e) ME.

Figure S7. Typical absorption spectra for monitoring the catalytic oxidation of OPD in the presence of AuPtRu nanozymes with various concentrations of (a) GSH, (b) DTT, (c) MS, (d) MA, and (e) ME.

Figure S8. Normalized peroxidase-like activity of AuPt nanozyme after incubation with different concentrations of the six biothiols (a) GSH, (b) Cys, (c) MA, (d) MS, (e) DTT, and (f) ME. Each error bar shows the standard deviation of five independent measurements.

Figure S9. Normalized peroxidase-like activity of AuPtRu nanozyme after incubation with different concentrations of the six biothiols (a) GSH, (b) Cys, (c) MA, (d) MS, (e) DTT, and (f) ME. Each error bar shows the standard deviation of five independent measurements.

Figure S10. Colorimetric response patterns ($(A_0\text{-}A)\ /A_0$) of nanozyme sensor arrays towards 5 μM of biothiols. Each error bar shows the standard deviation of five measurements. A and A_0 were the absorption of oxOPD in the presence and absence of biothiols in the nanozyme reaction systems, respectively. Each error bar shows the standard deviation of five independent measurements.

Figure S11. 2D canonical score plots for the first two factors of the colorimetric response patterns obtained against (a) 50 μM, (b) 20 μM, (c) 10 μM, and (d) 5 μM biothiols.

Table S1. Comparison of nanozyme-based assays for biothiol detection.

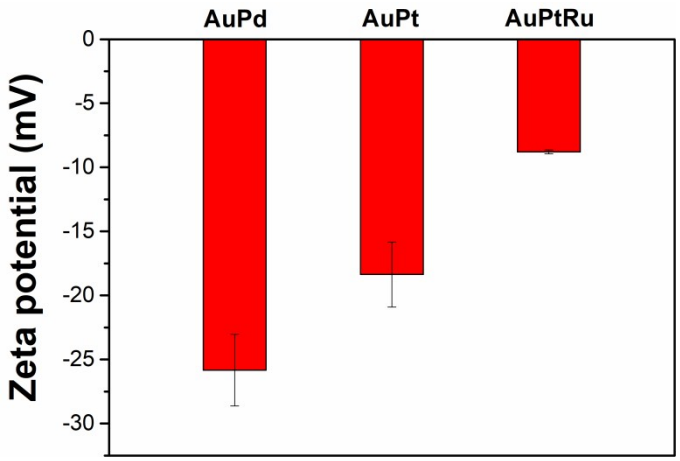

Figure S1. Zeta potentials of AuPd, AuPt, and AuPtRu. Each error bar shows the standard deviation of three independent measurements.

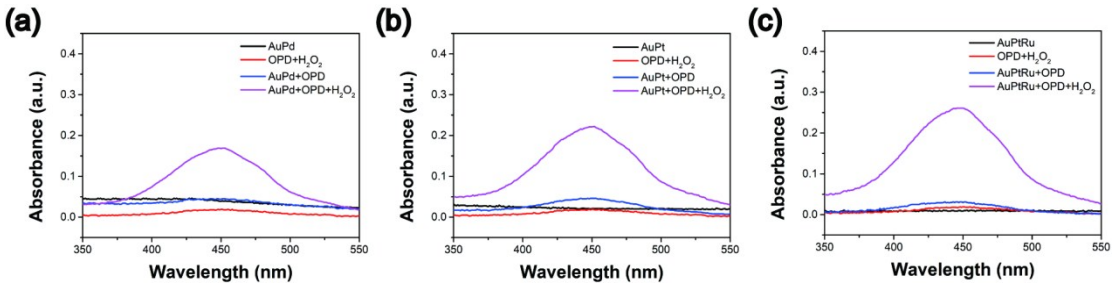

Figure S2. Absorption spectra of different reaction systems of (a) AuPd, (b) AuPt, and (c) AuPtRu nanozymes. Concentrations of OPD and H_2O_2 were 2 mM and 10 mM, respectively.

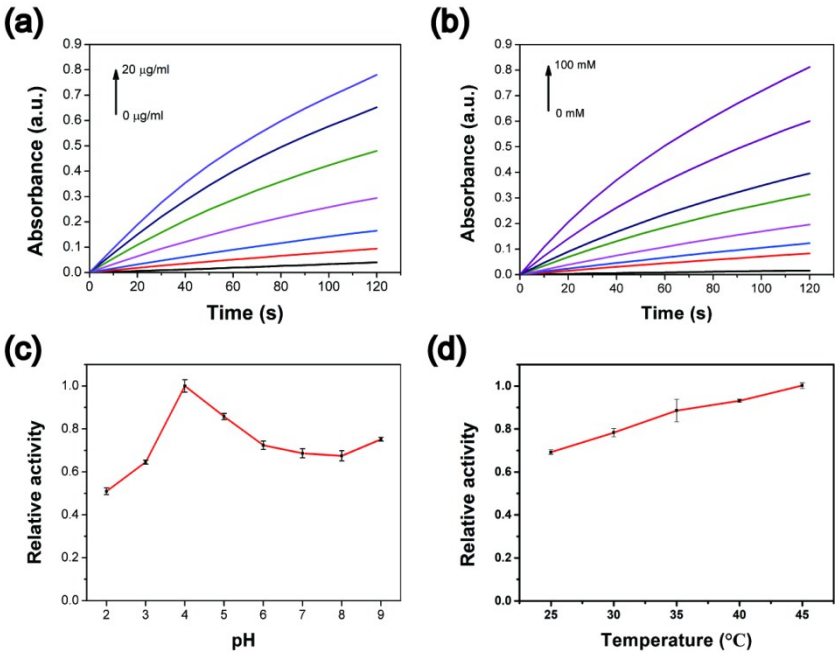

Figure S3. (a) Kinetic curves of A_{450} for monitoring the catalytic reaction of 2 mM OPD with various concentrations of AuPd nanozymes in the presence of 10 mM H_2O_2. (b) Kinetic curves of A_{450} for monitoring the catalytic reaction of 2 mM OPD with various concentrations of H_2O_2 in the presence of 5 μg/mL AuPd nanozymes. (c, d) pH and temperature dependent peroxidase-like activities of AuPd nanozymes. Each error bar shows the standard deviation of three independent measurements.

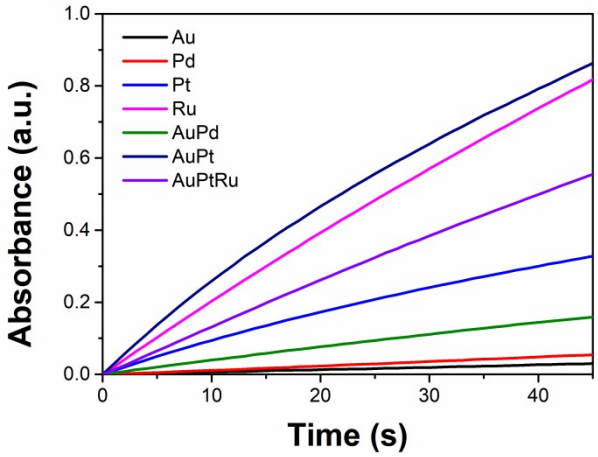

Figure S4. Kinetic curves of A_{450} for monitoring the catalytic reaction of 2 mM OPD and 10 mM H_2O_2 in the presence of 5 μg/mL different noble metal nanozymes.

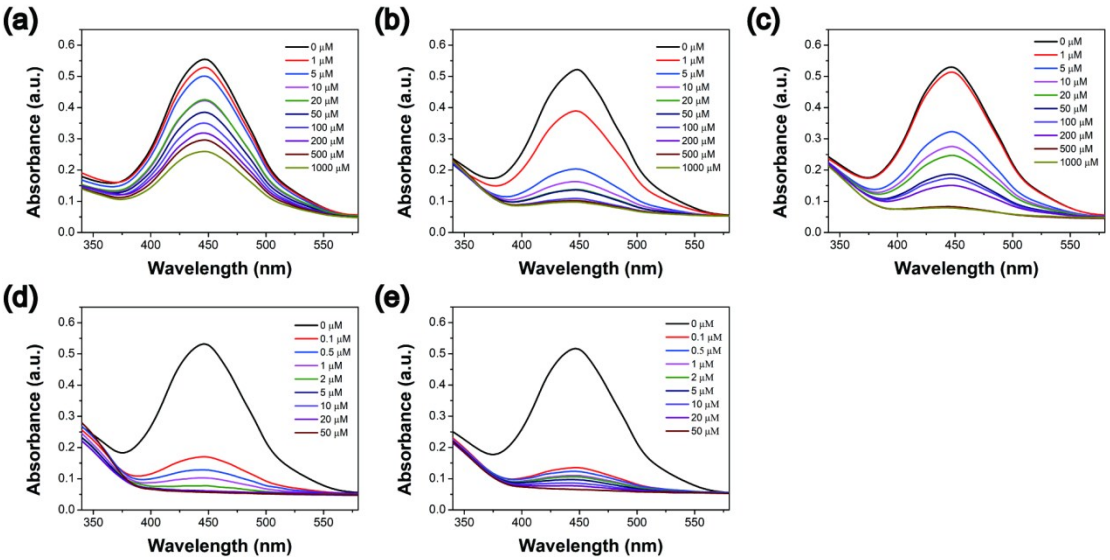

Figure S5. Typical absorption spectra for monitoring the catalytic oxidation of OPD in the presence of AuPd nanozymes with various concentrations of (a) GSH, (b) DTT, (c) MS, (d) MA, and (e) ME.

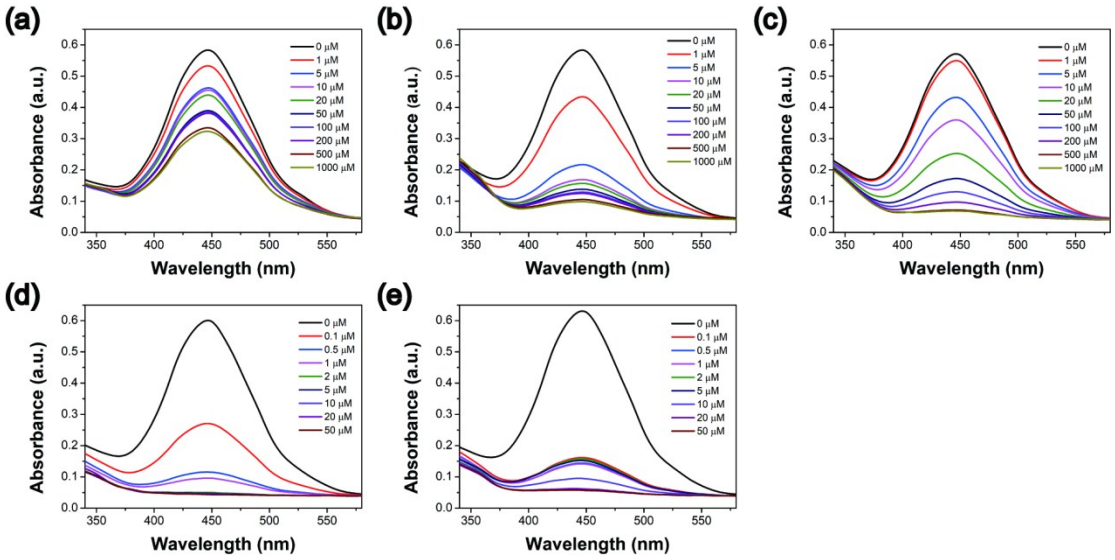

Figure S6. Typical absorption spectra for monitoring the catalytic oxidation of OPD in the presence of AuPt nanozymes with various concentrations of (a) GSH, (b) DTT, (c) MS, (d) MA, and (e) ME.

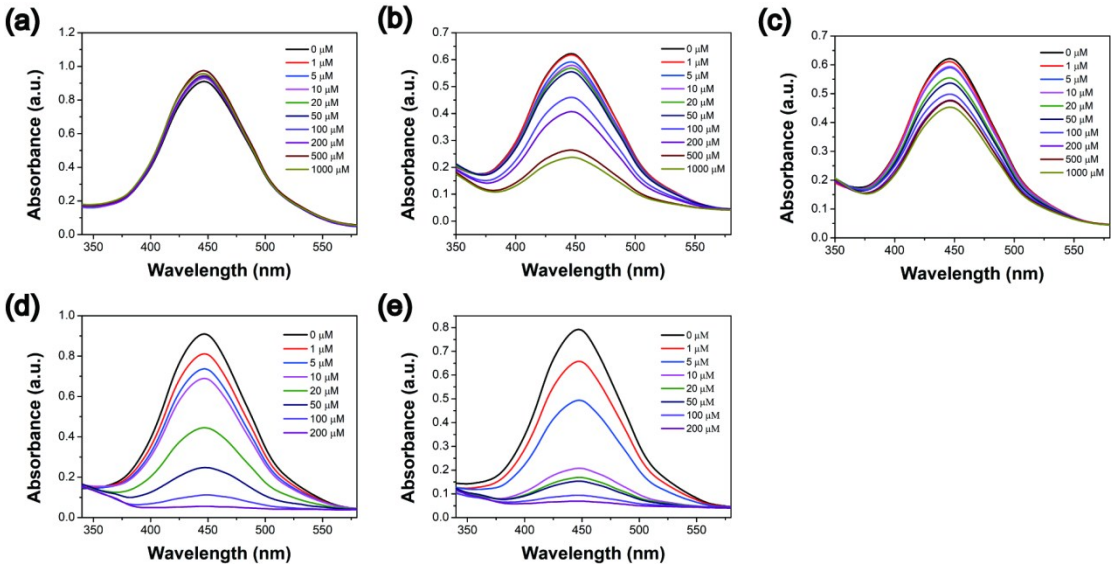

Figure S7. Typical absorption spectra for monitoring the catalytic oxidation of OPD in the presence of AuPtRu nanozymes with various concentrations of (a) GSH, (b) DTT, (c) MS, (d) MA, and (e) ME.

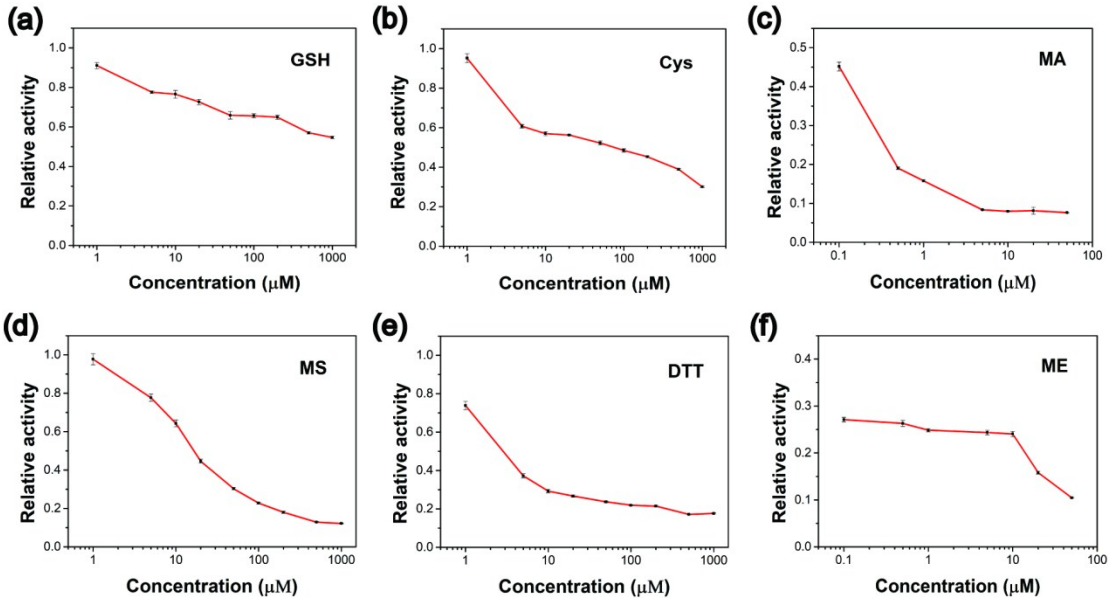

Figure S8. Normalized peroxidase-like activity of AuPt nanozyme after incubation with different concentrations of (a) GSH, (b) Cys, (c) MA, (d) MS, (e) DTT, and (f) ME. Each error bar shows the standard deviation of five independent measurements.

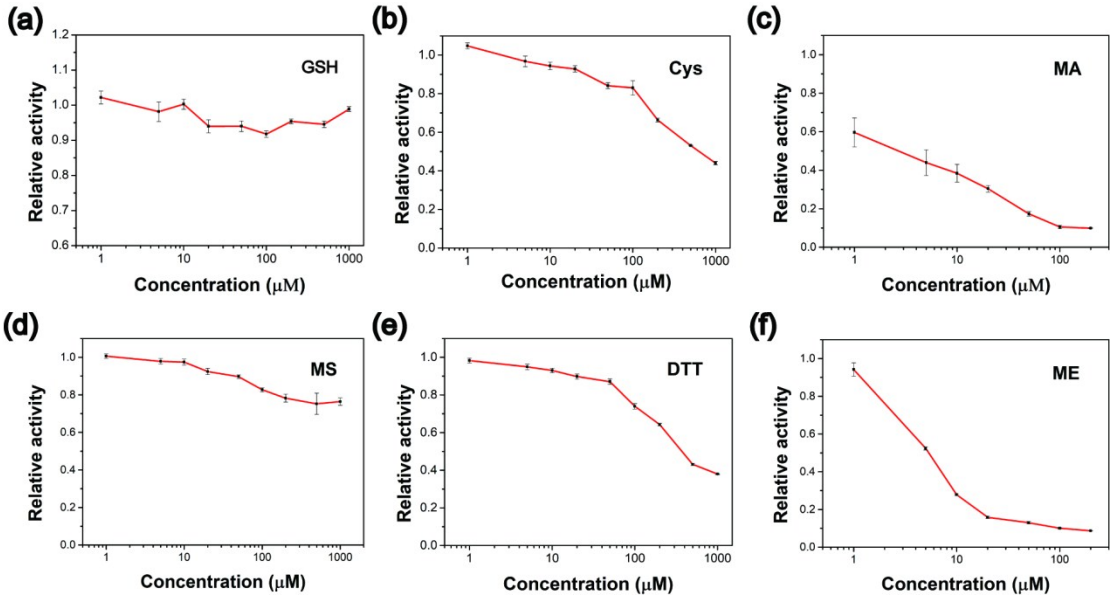

Figure S9. Normalized peroxidase-like activity of AuPtRu nanozyme after incubation with different concentrations of (a) GSH, (b) Cys, (c) MA, (d) MS, (e) DTT, and (f) ME. Each error bar shows the standard deviation of five independent measurements.

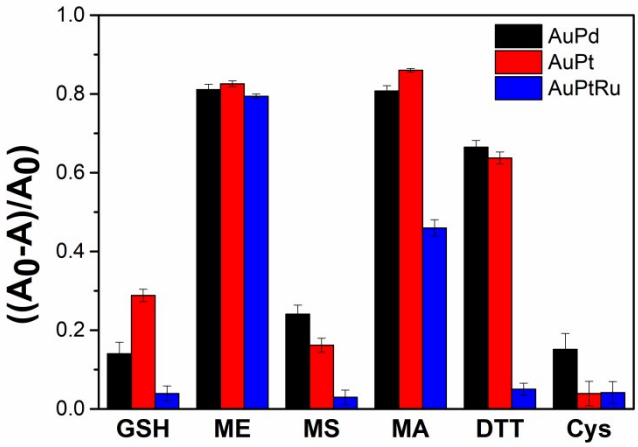

Figure S10. Colorimetric response patterns ($(A_0-A)/A_0$) of nanozyme sensor arrays towards 5 μM of biothiols. Each error bar shows the standard deviation of five measurements. A and A_0 were the absorption of oxOPD in the presence and absence of biothiols in the nanozyme reaction systems, respectively. Each error bar shows the standard deviation of five independent measurements.

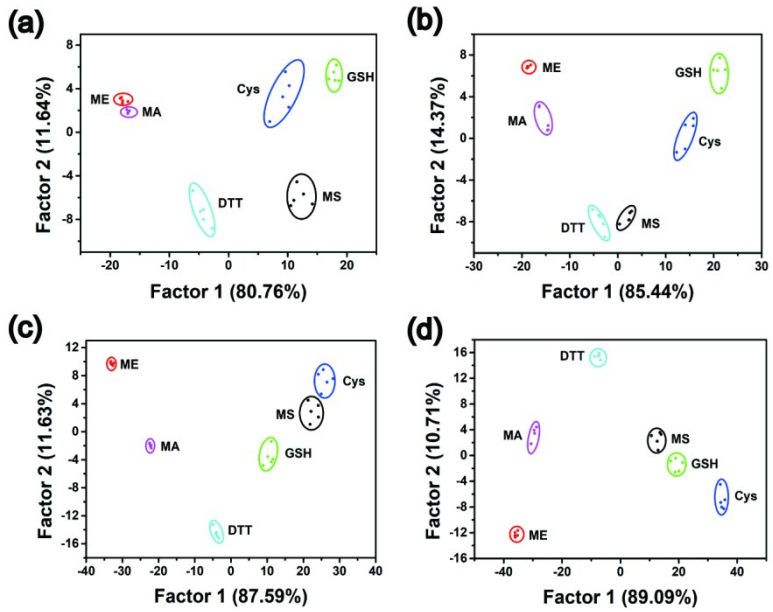

Figure S11. 2D canonical score plots for the first two factors of the colorimetric response patterns obtained against (a) 50 μM, (b) 20 μM, (c) 10 μM, and (d) 5 μM biothiols.

Table S1. Comparison of nanozyme-based assays for biothiol detection.

Methods	Nanozymes	Biothiols	Ref.
Fluorimetry	C-dots–MnO_2	GSH	[1]
Fluorimetry	ZIF-67	Cys	[2]
Colorimetry	MoS_2-PPy-Pd	Cys	[3]
Colorimetry	$FeMnO_3$	GSH	[4]
Colorimetry	Fe_3C/N−C	Cys	[5]
Colorimetry	V_2O_5	GSH	[6]
Colorimetry	Ce-MOF	GSH, Hcy, Cys	[7]
Colorimetry	Mn-Co nanosheets	GSH	[8]
Colorimetry	Co, N-HPC	GSH	[9]
Colorimetry	gold nanoclusters	GSH	[10]
Sensor array	Pt, Ru, Ir	GSH, Cys, DTT, MS, MA, ME	[11]
Sensor array	AuPd, AuPt, AuPtRu	GSH, Cys, DTT, MS, MA, ME	This work

References

1. Q. Y. Cai, J. Li, J. Ge, L. Zhang, Y. L. Hu, Z. H. Li and L. B. Qu, *Biosens. Bioelectron.*, 2015, **72**, 31-36.
2. T. Jin, Y. L. Li, W. J. Jing, Y. C. Li, L. Z. Fan and X. H. Li, *Chem. Commun.*, 2020, **56**, 659-662.
3. M. Q. Chi, Y. Zhu, L. W. Jing, C. Wang and X. F. Lu, *Anal. Chim. Acta*, 2018, **1035**, 146-153.
4. M. Q. Chi, S. H. Chen, M. X. Zhong, C. Wang and X. F. Lu, *Chem. Commun.*, 2018, **54**, 5827-5830.
5. N. Song, F. Q. Ma, Y. Zhu, S. H. Chen, C. Wang and X. F. Lu, *ACS Sustainable Chem. Eng.*, 2018, **6**, 16766-16776.
6. A. B. Ganganboina and R. A. Doong, *Sens. Actuators B Chem.*, 2018, **273**, 1179-1186.
7. Y. H. Xiong, S. H. Chen, F. G. Ye, L. J. Su, C. Zhang, S. F. Shen and S. L. Zhao, *Chem. Commun.*, 2015, **51**, 4635-4638.
8. Y. Zhang, C. L. Dai, W. Liu, Y. Y. Wang, F. Ding, P. Zou, X. X. Wang, Q. B. Zhao and H. B. Rao, *Mikrochim. Acta*, 2019, **186**, 340.
9. S. Q. Li, L. T. Wang, X. D. Zhang, H. X. Chai and Y. M. Huang, *Sens. Actuators B Chem.*, 2018, **264**, 312-319.
10. J. Feng, P. Huang, S. Shi, K. Y. Deng and F. Y. Wu, *Anal. Chim. Acta*, 2017, **967**, 64-69.
11. X. Y. Wang, L. Qin, M. Zhou, Z. P. Lou and H. Wei, *Anal. Chem.*, 2018, **90**, 11696-11702.